SUPPORTING INFORMATION

Sex-specific Silencing of X-linked Genes by Xist RNA

Srimonta Gayen, Emily Maclary, Michael Hinten, and Sundeep Kalantry

Department of Human Genetics, University of Michigan Medical School, Ann Arbor, MI 48105

*Correspondence: kalantry@umich.edu

Running title: Sex-specific inactivation patterns upon Xist induction

Keywords: Tsix, Xist, X-inactivation, embryonic stem cells, epiblast stem cells.

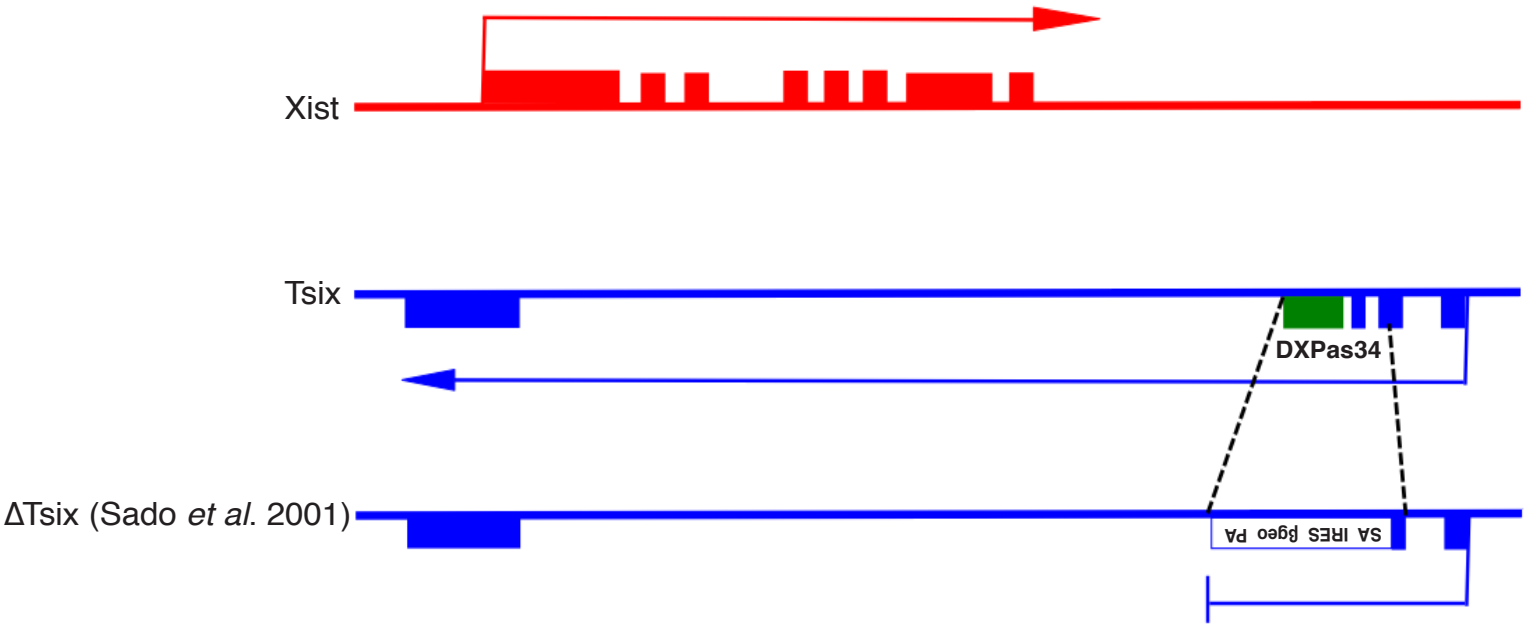
Xist
Tsix
DXPas34
ΔTsix (Sado *et al*. 2001)
SA IRES βgeo PA

Figure S1. Schematic representation of the Xist, Tsix, and the ΔTsix mutant loci. In the $X^{\Delta Tsix}$ mutation, the transcription of Tsix is terminated in exon 2 through insertion of an IRES-βgeo cassette containing an SV40 polyadenylation sequence (pA). The mutation also deletes exon 3 of Tsix and the Tsix enhancer *DXPas34* (1). Related to Fig. 1.

Fig. S2

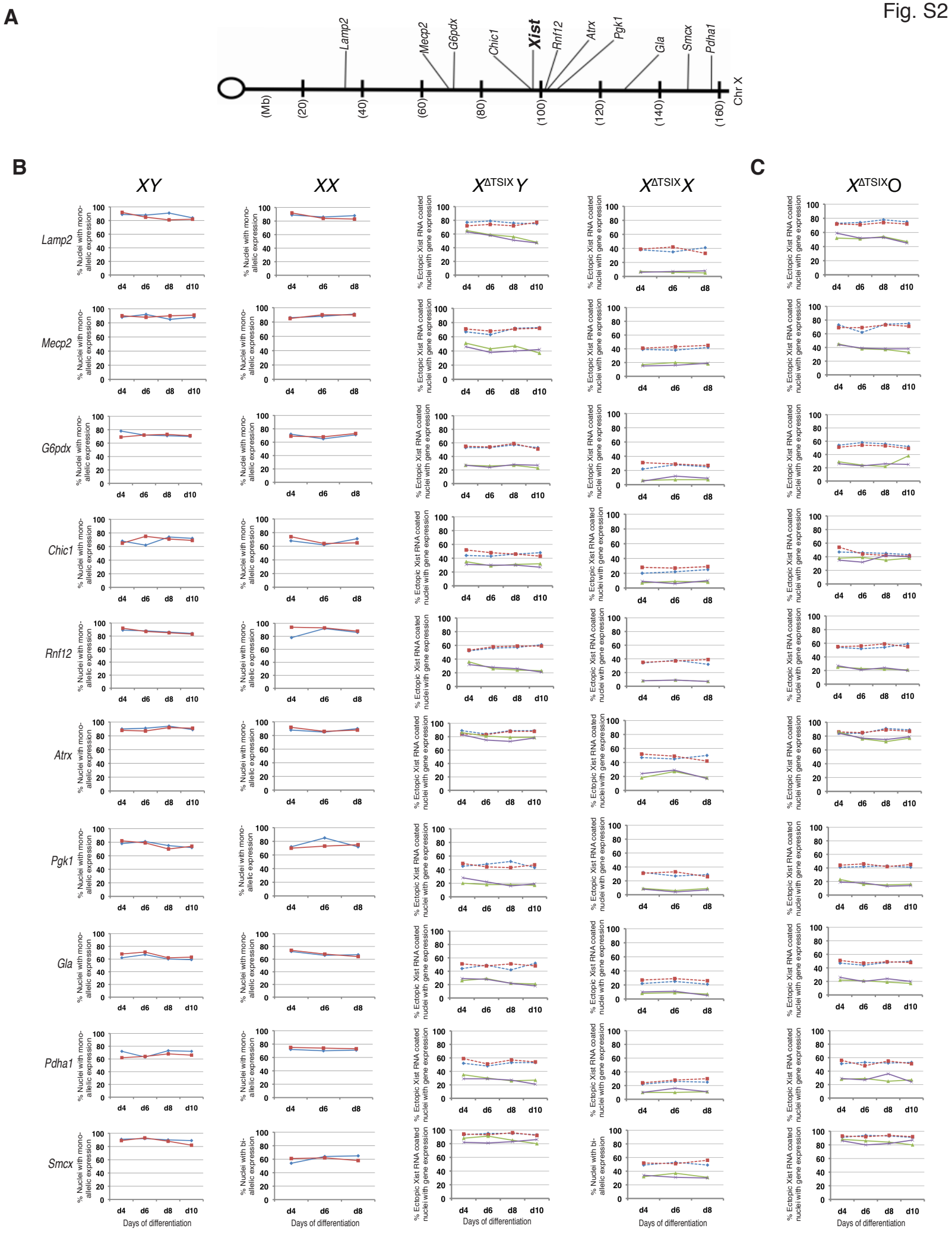
A
Lamp2
Mecp2
G6pdx
Chic1
Xist
Rnf12
Atrx
Pgk1
Gla
Smcx
Pdha1
(Mb)
(20)
(40)
(60)
(80)
(100)
(120)
(140)
(160)
Chr X
B
C
XY
XX
X^ΔTSIX Y
X^ΔTSIX X
X^ΔTSIX O
Lamp2
Mecp2
G6pdx
Chic1
Rnf12
Atrx
Pgk1
Gla
Pdha1
Smcx
% Nuclei with mono-allelic expression
% Nuclei with bi-allelic expression
% Ectopic Xist RNA coated nuclei with gene expression
d4
d6
d8
d10
Days of differentiation

Figure S2. Differential silencing of X-linked genes upon ectopic Xist RNA coating in differentiating $X^{\Delta Tsix}Y$, $X^{\Delta Tsix}X$, and $X^{\Delta Tsix}O$ ESCs. (A) X-chromosomal distribution of the genes profiled by RNA FISH. **(B)** Quantification of allelic expression of each of the ten genes in individual nuclei of differentiating *XY*, $X^{\Delta Tsix}Y$, *XX*, and $X^{\Delta Tsix}X$ ESC lines (two cell lines of each genotype). In WT *XY* and *XX* cells, % nuclei exhibiting monoallelic expression of genes from the active-X is plotted for all genes except *Smcx*. In mutant $X^{\Delta Tsix}Y$ and $X^{\Delta Tsix}X$ cells, monoallelic expression of the genes with coincident strong or weak ectopic Xist RNA coats (solid and dashed lines, respectively) is graphed for all genes except *Smcx*. *Smcx* escapes X-inactivation; thus, in female *XX* and $X^{\Delta Tsix}X$ nuclei biallelic expression of *Smcx* is quantified, while male *XY* and $X^{\Delta Tsix}Y$ plots show monoallelic expression. **(C)** Quantification of expression of the ten genes upon Xist RNA induction in individual nuclei of two differentiating $X^{\Delta Tsix}O$ ESC lines. For all cells, only nuclei harboring a single *Xist* locus in *XY*, $X^{\Delta Tsix}Y$, and $X^{\Delta Tsix}O$ cells or two *Xist* loci in *XX* and $X^{\Delta Tsix}X$ cells detected by DNA FISH were quantified. n=100 nuclei/cell line/day of differentiation. Related to Fig. 2.

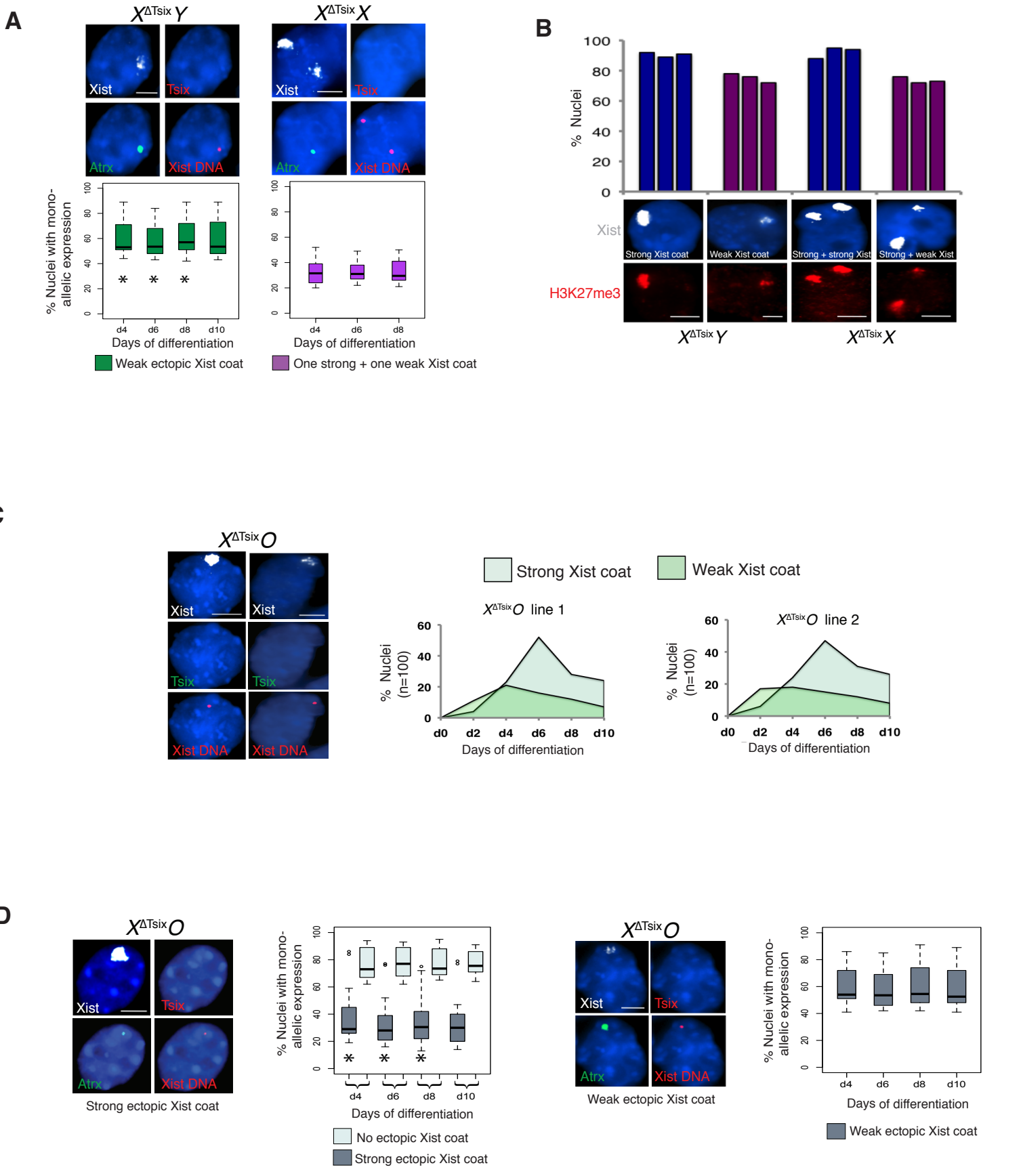
A
X^ΔTsix Y
X^ΔTsix X
Xist
Tsix
Atrx
Xist DNA
% Nuclei with mono-allelic expression
Days of differentiation
Weak ectopic Xist coat
One strong + one weak Xist coat
B
% Nuclei
Xist
Strong Xist coat
Weak Xist coat
Strong + strong Xist
Strong + weak Xist
H3K27me3
C
X^ΔTsix O
Strong Xist coat
Weak Xist coat
X^ΔTsix O line 1
X^ΔTsix O line 2
% Nuclei (n=100)
Days of differentiation
D
Strong ectopic Xist coat
No ectopic Xist coat
Weak ectopic Xist coat

Figure S3. Differential silencing of X-linked genes upon ectopic Xist RNA coating and H3-K27me3 enrichment in differentiating $X^{\Delta Tsix}Y$, $X^{\Delta Tsix}X$, and $X^{\Delta Tsix}O$ ESCs. **(A)** Boxplots of expression of the nine X-linked genes surveyed in Fig. 2 coincident with weak ectopic Xist RNA coats in the $X^{\Delta Tsix}Y$ and $X^{\Delta Tsix}X$ ESC lines analyzed in Fig. 2. For all cells, only nuclei harboring a single Xist locus in *XY* and $X^{\Delta Tsix}Y$ cells or two Xist loci in *XX* and $X^{\Delta Tsix}X$ cells by DNA FISH were quantified. n=100 nuclei/cell line/day of differentiation. *, $p < 0.003$, significant difference in gene expression between $X^{\Delta Tsix}Y$ and $X^{\Delta Tsix}X$ nuclei; Welch's two-sample T-test. **(B)** Enrichment of H3-K27me3 coincident with strong and weak ectopic Xist RNA coats in $X^{\Delta Tsix}Y$ and $X^{\Delta Tsix}X$ nuclei. Three different cell lines of each genotype quantified. n=100 nuclei/cell line/day of differentiation. **(C)** Quantification of Xist RNA coats in two differentiating $X^{\Delta Tsix}O$ ESC lines. **(D)** Boxplots of expression of all nine X-linked genes coincident with strong (left) and weak (right) Xist RNA coats in the $X^{\Delta Tsix}O$ ESC lines. n=100 nuclei/cell line/day of differentiation for each class of Xist RNA-coated cells. *, $p < 0.003$, significant difference in gene expression between $X^{\Delta Tsix}Y$ and $X^{\Delta Tsix}X$ nuclei by Welch's two-sample T-test. X-linked gene expression does not differ significantly between $X^{\Delta Tsix}O$ and $X^{\Delta Tsix}X$ nuclei lacking ectopic Xist coats ($p > 0.2$). Only nuclei with a single Xist locus in *XY*, $X^{\Delta Tsix}Y$, and $X^{\Delta Tsix}O$ cells or two Xist loci in *XX* and $X^{\Delta Tsix}X$ cells detected by DNA FISH were quantified. Scale bar, 2μM. Related to Fig. 2.

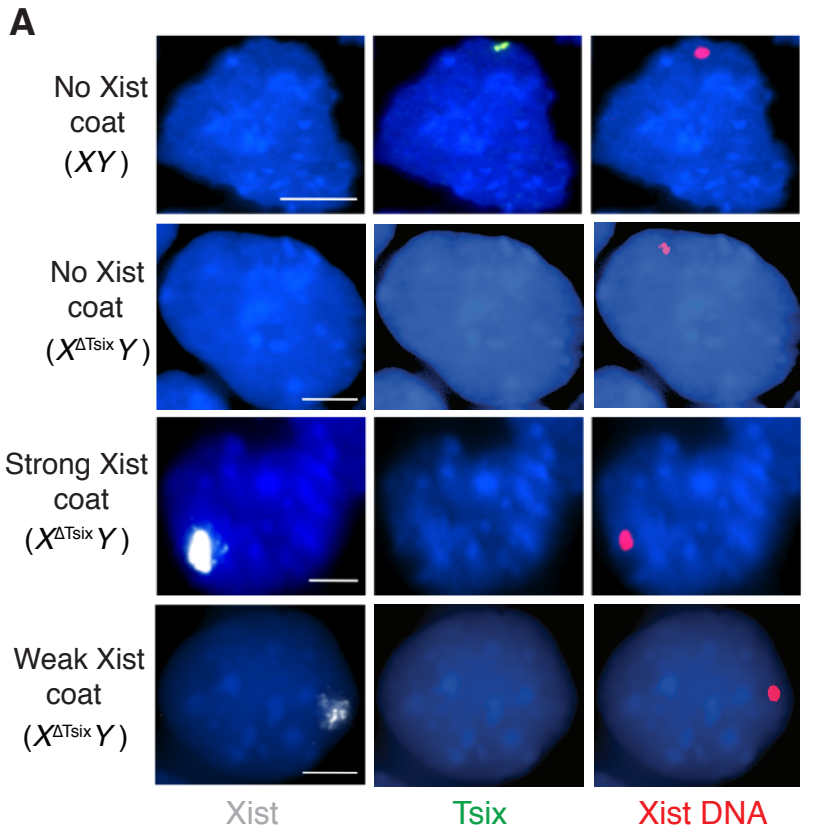
A
No Xist coat (XY)
No Xist coat ($X^{\Delta Tsix}Y$)
Strong Xist coat ($X^{\Delta Tsix}Y$)
Weak Xist coat ($X^{\Delta Tsix}Y$)
Xist
Tsix
Xist DNA

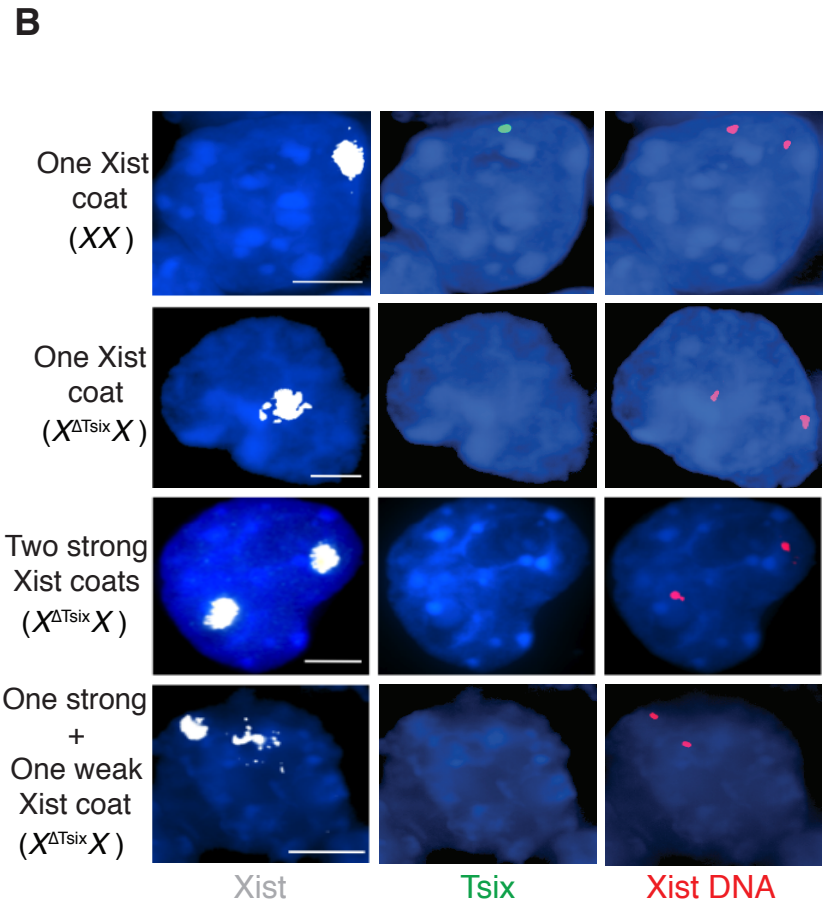
B
One Xist coat (XX)
One Xist coat ($X^{\Delta Tsix}X$)
Two strong Xist coats ($X^{\Delta Tsix}X$)
One strong + One weak Xist coat ($X^{\Delta Tsix}X$)
Xist
Tsix
Xist DNA

Figure S4. Differential ectopic Xist RNA coating in differentiating $X^{\Delta Tsix}Y$ vs. $X^{\Delta Tsix}X$ EpiSCs. RNA FISH detection of Xist (white) and Tsix (green) RNAs followed by Xist DNA FISH (red) in representative *XY* and $X^{\Delta Tsix}Y$ **(A)** and *XX* and $X^{\Delta Tsix}X$ **(B)** differentiated EpiSCs without or with strong or weak Xist RNA coats. Nuclei are stained blue with DAPI. Scale bar, 2μM. Related to Fig. 3

Fig. S5

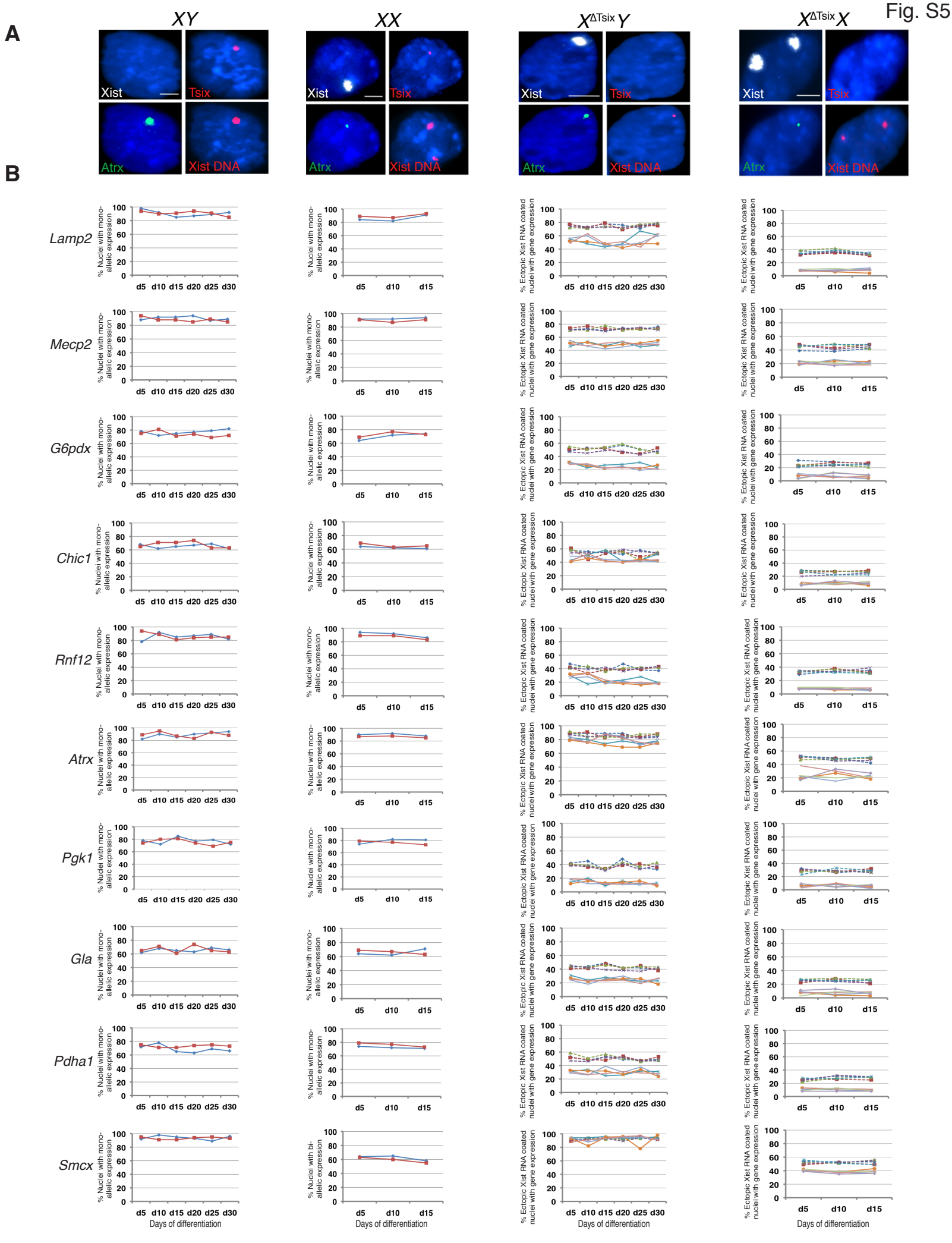
A
XY
XX
X^ΔTsix Y
X^ΔTsix X
Xist
Tsix
Atrx
Xist DNA
B
Lamp2
Mecp2
G6pdx
Chic1
Rnf12
Atrx
Pgk1
Gla
Pdha1
Smcx
% Nuclei with mono-allelic expression
% Nuclei with bi-allelic expression
% Ectopic Xist RNA coated nuclei with gene expression
d5 d10 d15 d20 d25 d30
Days of differentiation

Figure S5. Differential silencing of X-linked genes upon ectopic Xist RNA coating in differentiating $X^{\Delta Tsix}Y$ vs. $X^{\Delta Tsix}X$ EpiSCs. (A) Representative nucleus of each genotype stained to detect Xist RNA (white), Tsix RNA (red), and transcription of one of the 10 genes surveyed (Atrx, green) by RNA FISH. Following RNA FISH, the Xist locus was detected by DNA FISH. Nuclei are stained blue with DAPI. Scale bar, 2μM. **(B)** Quantification of allelic expression of each of ten genes in individual nuclei of differentiating *XY*, $X^{\Delta Tsix}Y$, *XX*, and $X^{\Delta Tsix}X$ EpiSC lines (2, 2, 4, and 5 lines, respectively). In WT female *XX* cells, % nuclei exhibiting monoallelic expression of genes from the active-X is plotted for all genes except *Smcx*. In mutant $X^{\Delta Tsix}Y$ and $X^{\Delta Tsix}X$ cells, monoallelic expression of the genes with coincident strong or weak ectopic Xist RNA coats (solid and dashed lines, respectively) is graphed for all genes except *Smcx*. *Smcx* escapes X-inactivation; thus, in *XX* and $X^{\Delta Tsix}X$ nuclei biallelic expression of *Smcx* is quantified, while male *XY* and $X^{\Delta Tsix}Y$ plots show monoallelic expression. Only nuclei harboring a single *Xist* locus in males or two *Xist* loci in females by DNA FISH were quantified. *n*=100 nuclei/cell line/day of differentiation. Related to Fig. 4.

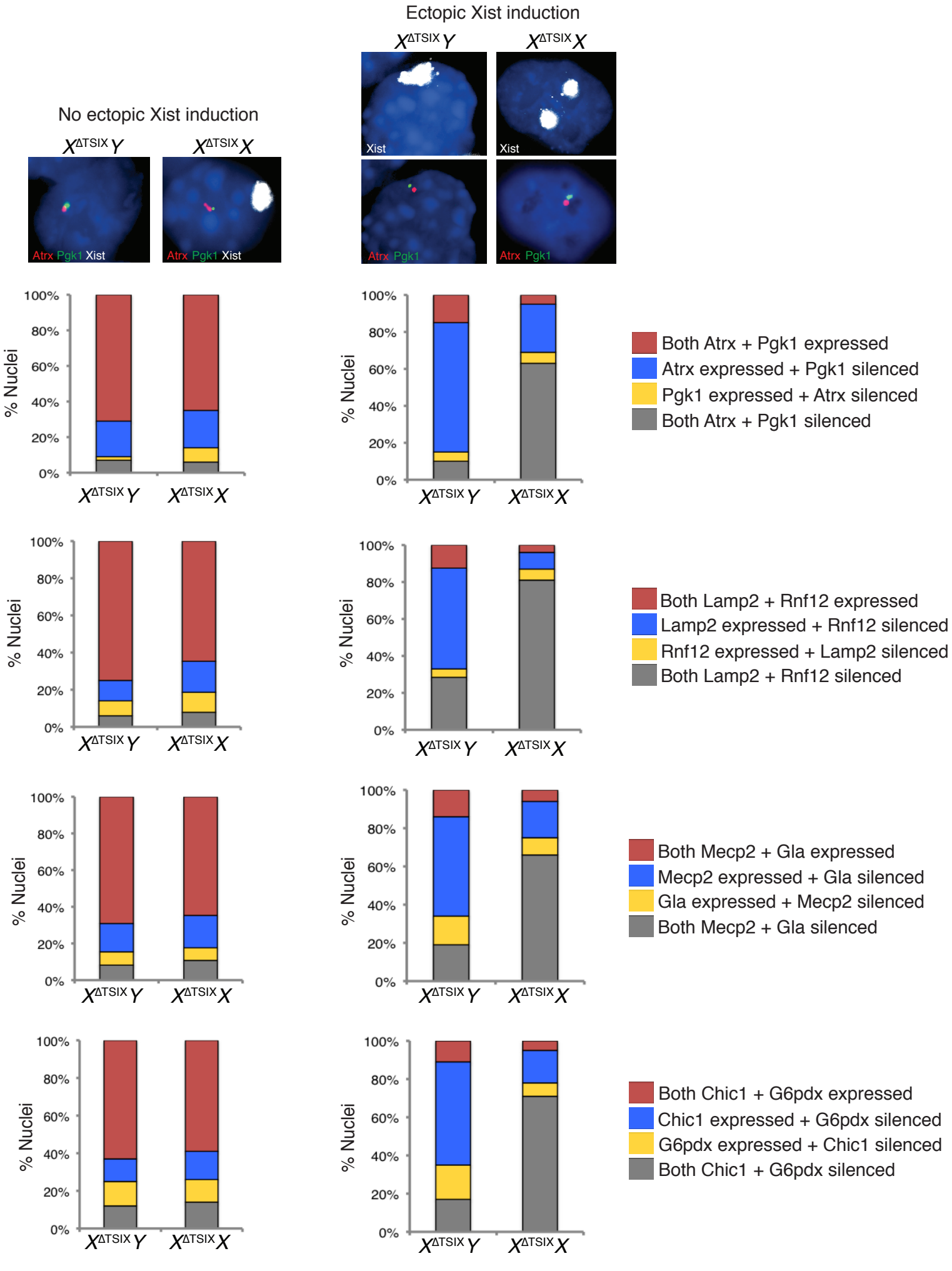
Ectopic Xist induction
$X^{\Delta TSIX}Y$
$X^{\Delta TSIX}X$
No ectopic Xist induction
$X^{\Delta TSIX}Y$
$X^{\Delta TSIX}X$
Xist
Atrx Pgk1 Xist
Atrx Pgk1
% Nuclei
100%
80%
60%
40%
20%
0%
Both Atrx + Pgk1 expressed
Atrx expressed + Pgk1 silenced
Pgk1 expressed + Atrx silenced
Both Atrx + Pgk1 silenced
Both Lamp2 + Rnf12 expressed
Lamp2 expressed + Rnf12 silenced
Rnf12 expressed + Lamp2 silenced
Both Lamp2 + Rnf12 silenced
Both Mecp2 + Gla expressed
Mecp2 expressed + Gla silenced
Gla expressed + Mecp2 silenced
Both Mecp2 + Gla silenced
Both Chic1 + G6pdx expressed
Chic1 expressed + G6pdx silenced
G6pdx expressed + Chic1 silenced
Both Chic1 + G6pdx silenced

Figure S6. Pairwise comparisons of X-linked gene expression in differentiating $X^{\Delta Tsix}Y$ and $X^{\Delta Tsix}X$ EpiSCs. Top panels, representative images of epiblast nuclei stained to detect Xist, Atrx, and Pgk1 RNAs. Plots assess gene expression of four pairs of genes in nuclei without (left) and with (right) ectopic Xist RNA coating. In the same nucleus, the two genes in any given pair are discordantly silenced more frequently in differentiating mutant $X^{\Delta Tsix}Y$ vs. $X^{\Delta Tsix}X$ EpiSCs ($p < 0.0001$, Fisher's exact test). In nuclei with ectopic Xist RNA coating, all genes except *Pgk1* were significantly more often silenced in females vs. males ($p << 0.001$ for *Atrx*, *Mecp2*, *Lamp2*, and *Chic1*; $p < 0.01$ for *Rnf12* and *G6pdx*; $p < 0.03$ for *Gla*; for *Pgk1*, $p = 0.12$; Fisher's exact test). Related to Fig. 4.

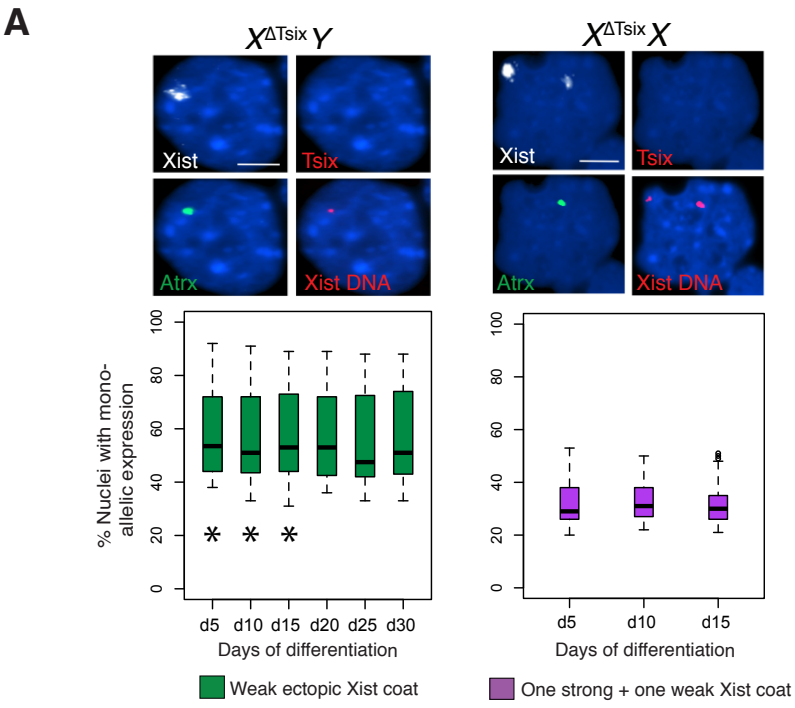
A
$X^{\Delta Tsix}Y$
$X^{\Delta Tsix}X$
Xist
Tsix
Atrx
Xist DNA
% Nuclei with mono-allelic expression
0
20
40
60
80
100
d5
d10
d15
d20
d25
d30
Days of differentiation
Weak ectopic Xist coat
One strong + one weak Xist coat

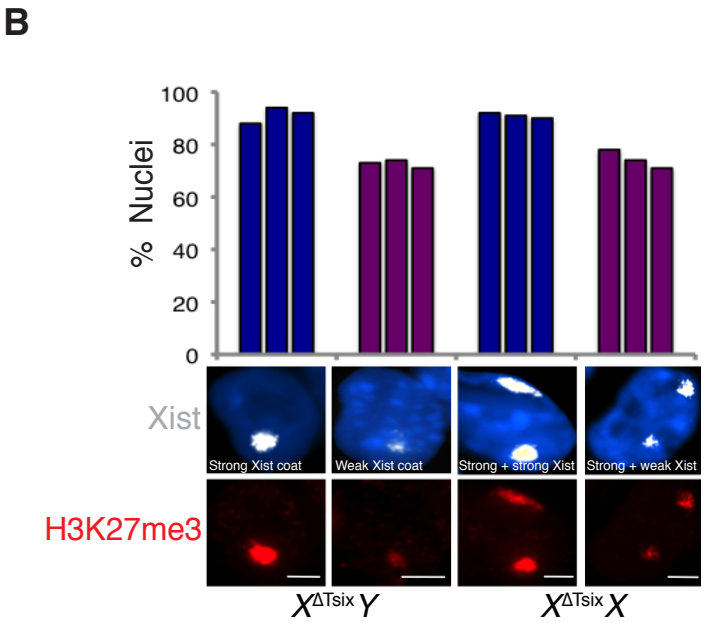
B
% Nuclei
0
20
40
60
80
100
Xist
H3K27me3
Strong Xist coat
Weak Xist coat
Strong + strong Xist
Strong + weak Xist
$X^{\Delta Tsix}Y$
$X^{\Delta Tsix}X$

Figure S7. Differential silencing of X-linked genes upon weak ectopic Xist RNA coating and H3-K27me3 enrichment in differentiating $X^{\Delta Tsix}Y$ vs. $X^{\Delta Tsix}X$ EpiSCs. **(A)** Boxplots of expression of the nine X-linked genes surveyed as in Figs. 2 and 4 coincident with weak ectopic Xist RNA coats in the $X^{\Delta Tsix}Y$ and $X^{\Delta Tsix}X$ EpiSC lines analyzed in Fig. 4. n=100 nuclei/cell line/day of differentiation. *, $p < 1 \times 10^{-6}$, significant difference in gene expression between $X^{\Delta Tsix}Y$ and $X^{\Delta Tsix}X$ nuclei; Welch's two-sample T-test. For all cells, only nuclei harboring a single *Xist* locus in *XY* and $X^{\Delta Tsix}Y$ cells or two *Xist* loci in *XX* and $X^{\Delta Tsix}X$ cells by DNA FISH were quantified. **(B)** Enrichment of H3-K27me3 coincident with strong and weak ectopic Xist RNA coats in $X^{\Delta Tsix}Y$ and $X^{\Delta Tsix}X$ nuclei. Three different cell lines of each genotype quantified. n=100 nuclei/cell line/day of differentiation. Scale bar, 2μM. Related to Fig. 4.

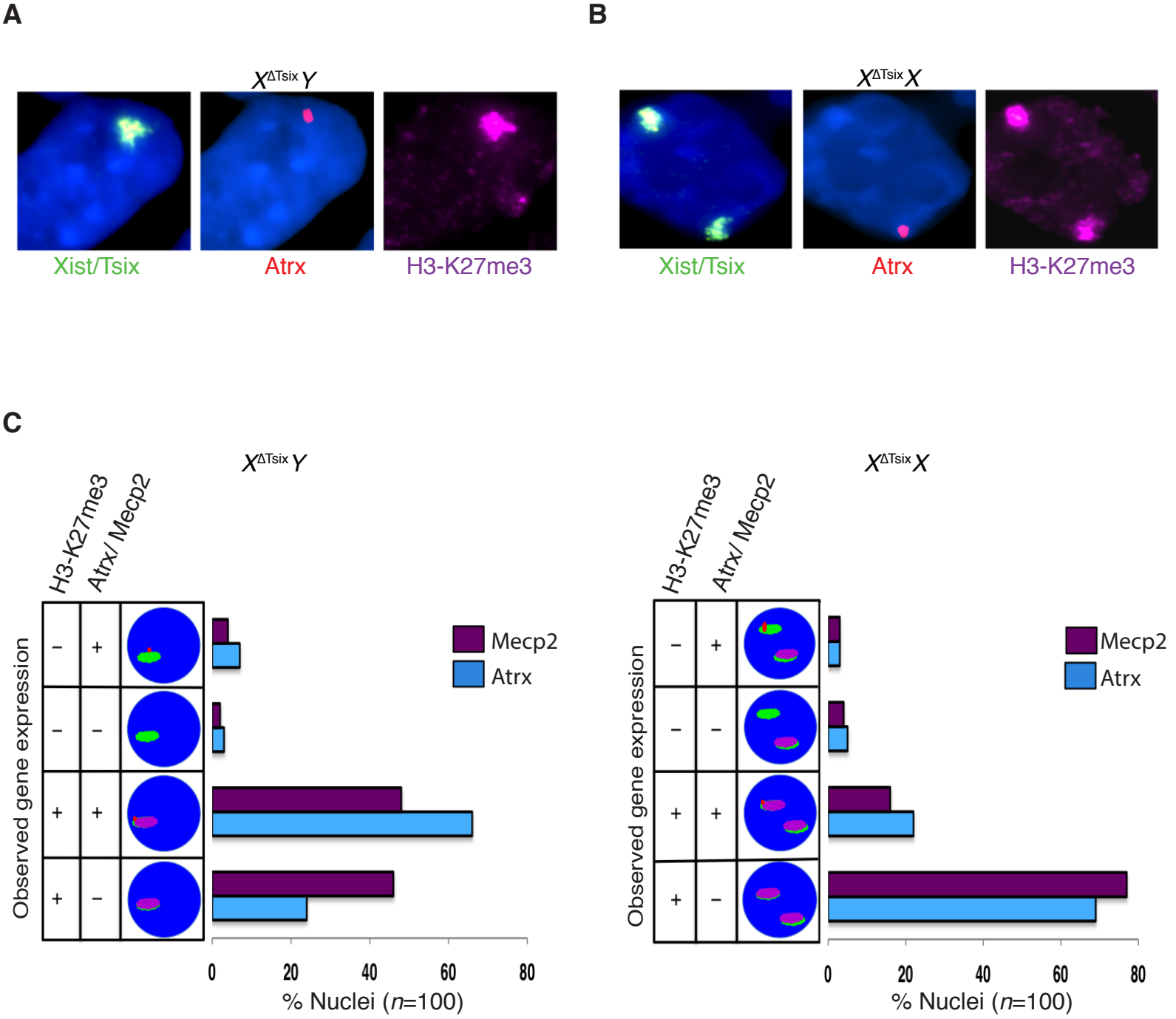
A
$X^{\Delta Tsix}Y$
Xist/Tsix
Atrx
H3-K27me3
B
$X^{\Delta Tsix}X$
Xist/Tsix
Atrx
H3-K27me3
C
$X^{\Delta Tsix}Y$
H3-K27me3
Atrx/ Mecp2
Observed gene expression
Mecp2
Atrx
0
20
40
60
80
% Nuclei (n=100)
$X^{\Delta Tsix}X$
H3-K27me3
Atrx/ Mecp2
Observed gene expression
Mecp2
Atrx
0
20
40
60
80
% Nuclei (n=100)

Figure S8. Enrichment of H3-K27me3 and coincident gene expression on the X-chromosome in differentiating $X^{\Delta Tsix}Y$ and $X^{\Delta Tsix}X$ EpiSCs. (A-B) RNA FISH detection of Xist, Tsix and Atrx RNAs coupled with immunofluorescence detection of H3-K27me3 in representative differentiated male $X^{\Delta Tsix}Y$ **(A)** and female $X^{\Delta Tsix}X$ **(B)** EpiSC lines. Nuclei are stained blue with DAPI. **(C)** Quantification of expression of the X-linked genes *Atrx* and *Mecp2* and enrichment of H3-K27me3 on the X-chromosome. Whereas H3-K27me3 enrichment nearly always coincides with silencing of *Atrx* and *Mecp2* in females, it does so significantly less frequently in males (p <0.0001, Fisher's exact test). The X-axis of each graph represents the average percentage of nuclei in each class. Diagrams along the Y-axis depict all observed expression patterns. Related to Fig. 4.

Fig. S9

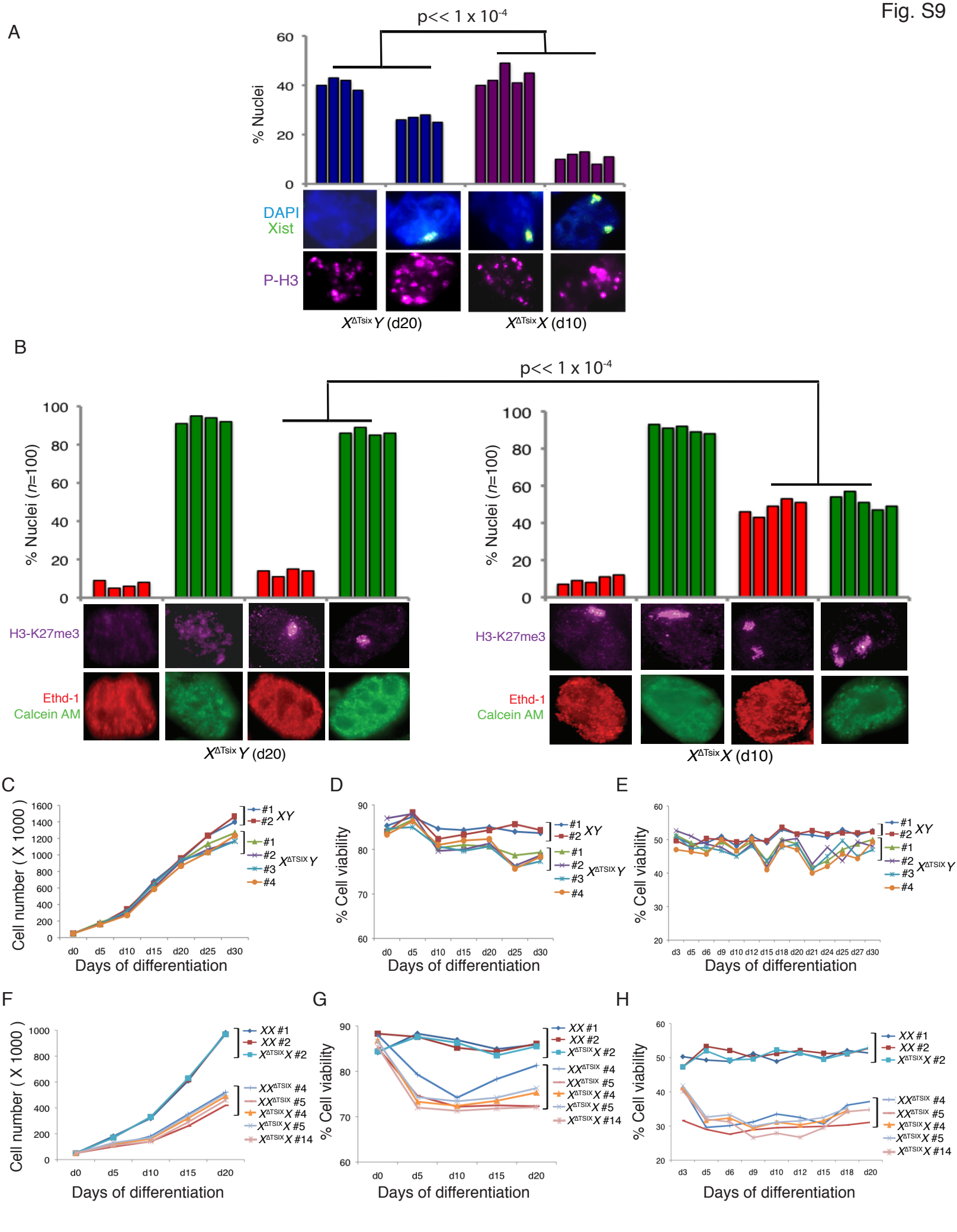
A
p<< 1 x 10-4
% Nuclei
DAPI
Xist
P-H3
XΔTsix Y (d20)
XΔTsix X (d10)
B
p<< 1 x 10-4
% Nuclei (n=100)
H3-K27me3
Ethd-1
Calcein AM
XΔTsix Y (d20)
XΔTsix X (d10)
C
Cell number (X 1000)
Days of differentiation
#1 #2 XY
#1 #2 #3 #4 XΔTSIX Y
D
% Cell viability
Days of differentiation
E
% Cell viability
Days of differentiation
F
Cell number (X 1000)
Days of differentiation
XX #1
XX #2
XΔTSIX X #2
XXΔTSIX #4
XXΔTSIX #5
XΔTSIX X #4
XΔTSIX X #5
XΔTSIX X #14
G
% Cell viability
Days of differentiation
H
% Cell viability
Days of differentiation

Figure S9. Differential cell proliferation and cell death in differentiating $X^{\Delta Tsix}Y$ vs. $X^{\Delta Tsix}X$ EpiSCs with ectopic Xist RNA coating. (A) Reduced phospho-H3 staining, a marker of cell proliferation, in differentiating mutant $X^{\Delta Tsix}Y$ and $X^{\Delta Tsix}X$ EpiSC lines (4 male and 5 female cell lines, as in Fig. 3) with and without ectopic Xist RNA coating. Mutant $X^{\Delta Tsix}Y$ and $X^{\Delta Tsix}X$ EpiSCs display maximal percentage of ectopically Xist RNA coated cells at d20 and d10 of differentiation, respectively (Fig. 3); thus, cell proliferation and viability (see panel **B**) were profiled at these two time points. n=100 nuclei for each of the four categories. p values calculated through Fisher's exact test. **(B)** Assessment of cell death in d20 and d10 differentiated mutant $X^{\Delta Tsix}Y$ and $X^{\Delta Tsix}X$ EpiSCs. H3-K27me3 accumulation (purple) serves to mark Xist RNA coated X-chromosomes (see Fig. S7). Ethd-1 (red) marks dead cells and Calcein AM (green) marks live cells. Compared to $X^{\Delta Tsix}Y$ males with ectopic H3-K27me3 accumulation, $X^{\Delta Tsix}X$ females with ectopic H3-K27me3 accumulation show a significantly higher level of cell death (p <<1 x 10-4, Welch's two-sample T-test). $X^{\Delta Tsix}Y$, lines 1-4; $X^{\Delta Tsix}X$, lines 4, 5, 14, and $XX^{\Delta Tsix}$ lines 4-5 (all assayed in Fig. 3). **(C)** Cell counts during the course of differentiation of XY and $X^{\Delta Tsix}Y$ male EpiSCs. **(D-E)** Viability of differentiating XY and $X^{\Delta Tsix}Y$ male EpiSCs. **D,** adherent cells; **E**, non-adherent cells in suspension. **(F)** Cell counts during differentiation of XX and $X^{\Delta Tsix}X$ / $XX^{\Delta Tsix}$ (by convention, the maternal allele precedes the paternal allele) female EpiSCs. **(G-H)** Reduced viability of differentiating XX and $X^{\Delta Tsix}X$ / $XX^{\Delta Tsix}$ female EpiSCs. **G**, adherent cells; **H**, non-adherent cells in suspension. The data in **C-H** are taken from ref. 7, except for the cell counts and viability of $X^{\Delta Tsix}X$ cell lines $X^{\Delta Tsix}X$ 4, 5 and 14. The greater the frequency of cells in undifferentiated $X^{\Delta Tsix}X$ / $XX^{\Delta Tsix}$ female EpiSCs that can ectopically express Xist during differentiation, i.e., cells that have originally chosen the $X^{\Delta Tsix}$ as the active-X, the larger the reduction in cell proliferation and viability. For example, in undifferentiated $X^{\Delta Tsix}X$ EpiSC line 2, the $X^{\Delta Tsix}$ is chosen as the inactive-X in all the cells at the onset of X-inactivation. This line therefore doesn't have any cells eligible to ectopically express Xist, hence it doesn't show any reduction in cell number or viability. Related to Fig. 4.

Fig. S10

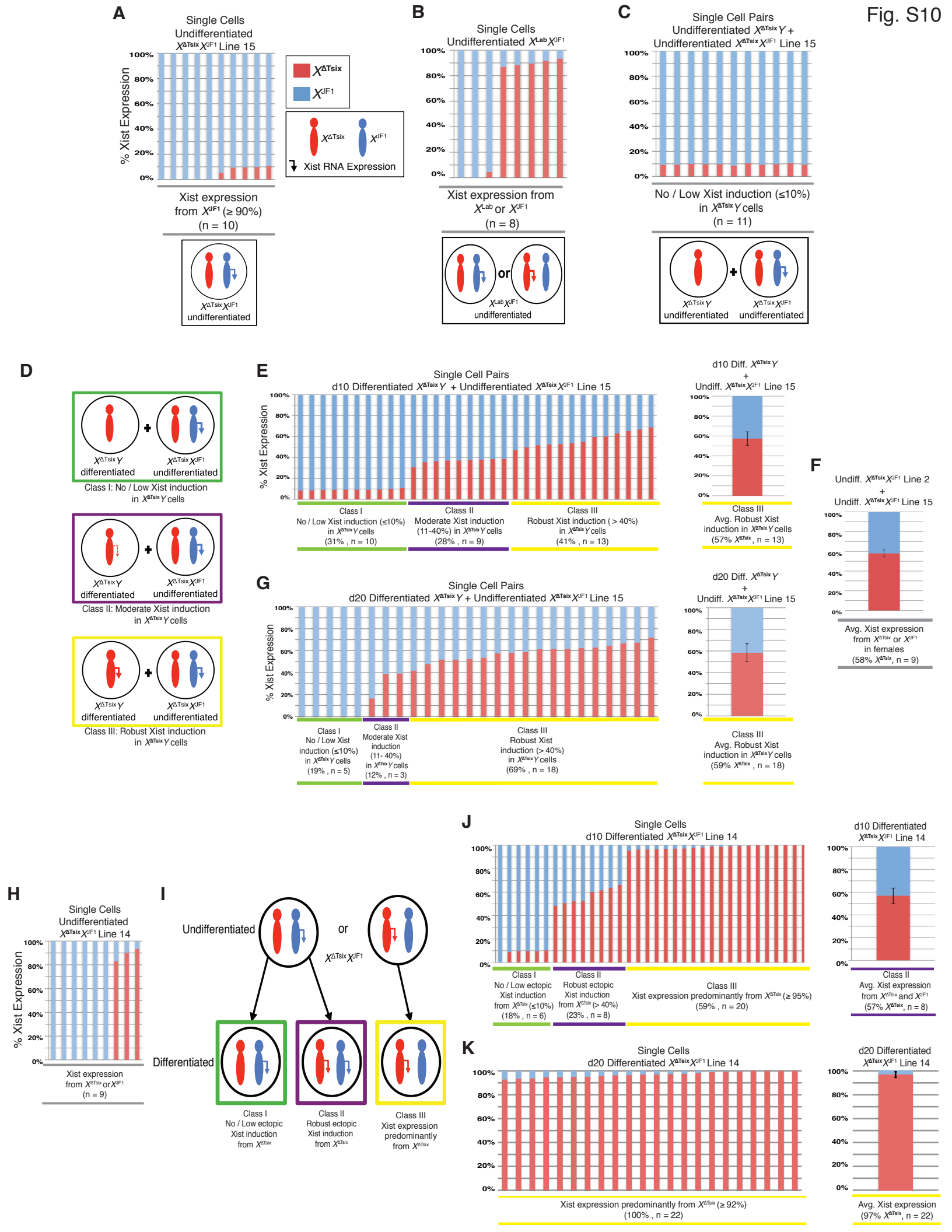
A
Single Cells
Undifferentiated
X^ΔTsix X^JF1 Line 15
% Xist Expression
100%
80%
60%
40%
20%
0%
X^ΔTsix
X^JF1
X^ΔTsix X^JF1
Xist RNA Expression
Xist expression
from X^JF1 (≥ 90%)
(n = 10)
X^ΔTsix X^JF1
undifferentiated
B
Single Cells
Undifferentiated X^Lab X^JF1
Xist expression from
X^Lab or X^JF1
(n = 8)
or
X^Lab X^JF1
undifferentiated
C
Single Cell Pairs
Undifferentiated X^ΔTsix Y +
Undifferentiated X^ΔTsix X^JF1 Line 15
No / Low Xist induction (≤10%)
in X^ΔTsix Y cells
(n = 11)
X^ΔTsix Y
undifferentiated
X^ΔTsix X^JF1
undifferentiated
D
X^ΔTsix Y
differentiated
X^ΔTsix X^JF1
undifferentiated
Class I: No / Low Xist induction
in X^ΔTsix Y cells
Class II: Moderate Xist induction
in X^ΔTsix Y cells
Class III: Robust Xist induction
in X^ΔTsix Y cells
E
Single Cell Pairs
d10 Differentiated X^ΔTsix Y + Undifferentiated X^ΔTsix X^JF1 Line 15
% Xist Expression
Class I
No / Low Xist induction (≤10%)
in X^ΔTsix Y cells
(31% , n = 10)
Class II
Moderate Xist induction
(11-40%) in X^ΔTsix Y cells
(28% , n = 9)
Class III
Robust Xist induction (> 40%)
in X^ΔTsix Y cells
(41% , n = 13)
d10 Diff. X^ΔTsix Y
+
Undiff. X^ΔTsix X^JF1 Line 15
Class III
Avg. Robust Xist
induction in X^ΔTsix Y cells
(57% X^ΔTsix , n = 13)
F
Undiff. X^ΔTsix X^JF1 Line 2
+
Undiff. X^ΔTsix X^JF1 Line 15
Avg. Xist expression
from X^ΔTsix or X^JF1
in females
(58% X^ΔTsix, n = 9)
G
Single Cell Pairs
d20 Differentiated X^ΔTsix Y + Undifferentiated X^ΔTsix X^JF1 Line 15
% Xist Expression
Class I
No / Low Xist
induction (≤10%)
in X^ΔTsix Y cells
(19% , n = 5)
Class II
Moderate Xist
induction
(11- 40%)
in X^ΔTsix Y cells
(12% , n = 3)
Class III
Robust Xist
induction (> 40%)
in X^ΔTsix Y cells
(69% , n = 18)
d20 Diff. X^ΔTsix Y
+
Undiff. X^ΔTsix X^JF1 Line 15
Class III
Avg. Robust Xist
induction in X^ΔTsix Y cells
(59% X^ΔTsix , n = 18)
H
Single Cells
Undifferentiated
X^ΔTsix X^JF1 Line 14
% Xist Expression
Xist expression
from X^ΔTsix or X^JF1
(n = 9)
I
Undifferentiated
or
X^ΔTsix X^JF1
Differentiated
Class I
No / Low ectopic
Xist induction
from X^ΔTsix
Class II
Robust ectopic
Xist induction
from X^ΔTsix
Class III
Xist expression
predominantly
from X^ΔTsix
J
Single Cells
d10 Differentiated X^ΔTsix X^JF1 Line 14
Class I
No / Low ectopic
Xist induction
from X^ΔTsix (≤10%)
(18% , n = 6)
Class II
Robust ectopic
Xist induction
from X^ΔTsix (> 40%)
(23% , n = 8)
Class III
Xist expression predominantly from X^ΔTsix (≥ 95%)
(59% , n = 20)
d10 Differentiated
X^ΔTsix X^JF1 Line 14
Class II
Avg. Xist expression
from X^ΔTsix and X^JF1
(57% X^ΔTsix, n = 8)
K
Single Cells
d20 Differentiated X^ΔTsix X^JF1 Line 14
Xist expression predominantly from X^ΔTsix (≥ 92%)
(100% , n = 22)
d20 Differentiated
X^ΔTsix X^JF1 Line 14
Avg. Xist expression
(97% X^ΔTsix, n = 22)

Figure S10. Xist RNA expression in individual undifferentiated $X^{\Delta Tsix}Y$ and $X^{\Delta Tsix}X$ EpiSCs. **(A)** Preferential expression of Xist from the X^{JF1} in single cells from an $X^{\Delta Tsix}X^{JF1}$ EpiSC line (line 15) with biased X-inactivation. Each bar represents a single cell. Xist RNA originating from the X^{Lab} or $X^{\Delta Tsix}$ is distinguished from the X^{JF1} by a SNP whose relative abundance is quantified by Pyrosequencing of the amplified cDNA. **(B)** Allelic expression of Xist RNA in single undifferentiated WT $X^{Lab}X^{JF1}$ EpiSC cells. **(C)** Quantification of Xist induction in undifferentiated $X^{\Delta Tsix}Y$ EpiSCs. Single $X^{\Delta Tsix}Y$ EpiSCs were combined with single undifferentiated $X^{\Delta Tsix}X^{JF1}$ line 15 EpiSCs, followed by Xist RT-PCR and Pyrosequencing. **(D)** Schematic of possible Xist induction patterns in individual differentiated $X^{\Delta Tsix}Y$ EpiSCs, measured by combining single $X^{\Delta Tsix}Y$ cells with single undifferentiated $X^{\Delta Tsix}X^{JF1}$ line 15 EpiSCs. **(E)** Quantification of Xist expression from the $X^{\Delta Tsix}$ in day (d) 10 differentiated $X^{\Delta Tsix}Y$ EpiSCs relative to Xist expression from the X^{JF1} in undifferentiated $X^{\Delta Tsix}X^{JF1}$ line 15 EpiSCs. **(F)** Average Xist expression from the $X^{\Delta Tsix}$ and X^{JF1} in female EpiSCs, measured by combining single cells from the $X^{\Delta Tsix}X^{JF1}$ EpiSC line 15, which expresses Xist almost exclusively from the X^{JF1} with single cells from the $X^{\Delta Tsix}X^{JF1}$ EpiSC line 2, which expresses Xist only from the $X^{\Delta Tsix}$ (2). The average Xist expression from the $X^{\Delta Tsix}$ allele in robustly Xist expressing Class III $X^{\Delta Tsix}Y$ cells at d10, shown in panel **E** matches the average Xist expression from the $X^{\Delta Tsix}$ allele in $X^{\Delta Tsix}X^{JF1}$ females (57% vs. 58%). **(G)** Quantification of Xist expression from the $X^{\Delta Tsix}$ in day (d) 20 differentiated $X^{\Delta Tsix}Y$ EpiSCs relative to Xist expression from the X^{JF1} in undifferentiated $X^{\Delta Tsix}X^{JF1}$ line 15 EpiSCs. As with d10 $X^{\Delta Tsix}Y$ cells, the average Xist expression from the $X^{\Delta Tsix}$ allele in robustly Xist expressing Class III $X^{\Delta Tsix}Y$ cells at d20 matches the average Xist expression from the $X^{\Delta Tsix}$ allele in $X^{\Delta Tsix}X^{JF1}$ females (59% vs. 58%). **(H)** Allelic Xist expression in single undifferentiated $X^{\Delta Tsix}X^{JF1}$ line 14 EpiSCs. **(I)** Schematic of expected Xist induction patterns in differentiated $X^{\Delta Tsix}X^{JF1}$ EpiSCs. **(J)** Quantification of allelic Xist expression in individual d10 differentiated $X^{\Delta Tsix}X^{JF1}$ line 14 EpiSCs. **(K)** Quantification of allelic Xist expression in individual d20 differentiated $X^{\Delta Tsix}X^{JF1}$ line 14 EpiSCs. At d20, only cells with exclusive or almost exclusive Xist expression from the $X^{\Delta Tsix}$ are found, due to reduced proliferation and/or death of cells that originally expressed Xist from the X^{JF1} and

which subsequently induced Xist from the $X^{\Delta Tsix}$ upon differentiation, resulting in silencing of genes on both Xs (see Fig. S9 and ref. (2)). Related to Fig. 5.

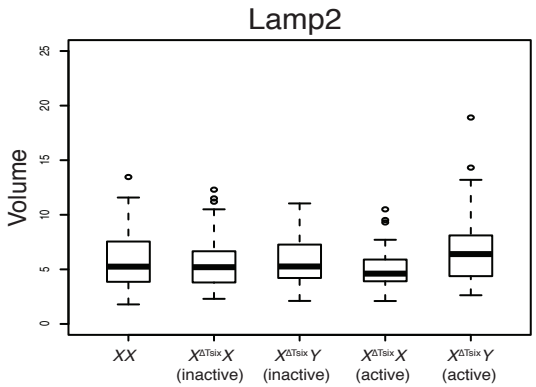
Lamp2
Volume
0
5
10
15
20
25
XX
X^ΔTsix X (inactive)
X^ΔTsix Y (inactive)
X^ΔTsix X (active)
X^ΔTsix Y (active)

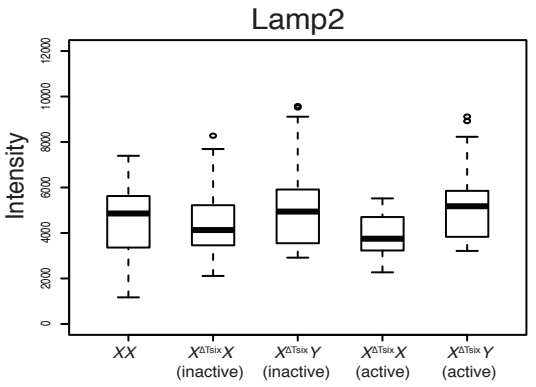
Lamp2
Intensity
0
2000
4000
6000
8000
10000
12000
XX
X^ΔTsix X (inactive)
X^ΔTsix Y (inactive)
X^ΔTsix X (active)
X^ΔTsix Y (active)

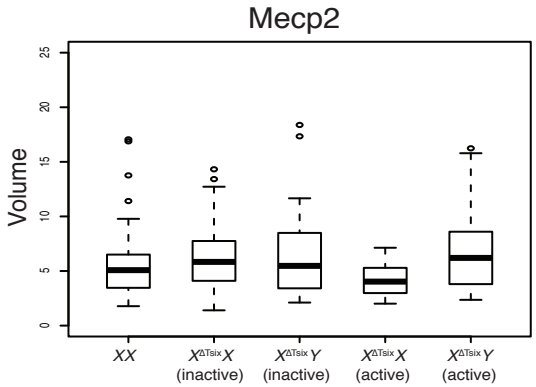
Mecp2
Volume
0
5
10
15
20
25
XX
X^ΔTsix X (inactive)
X^ΔTsix Y (inactive)
X^ΔTsix X (active)
X^ΔTsix Y (active)

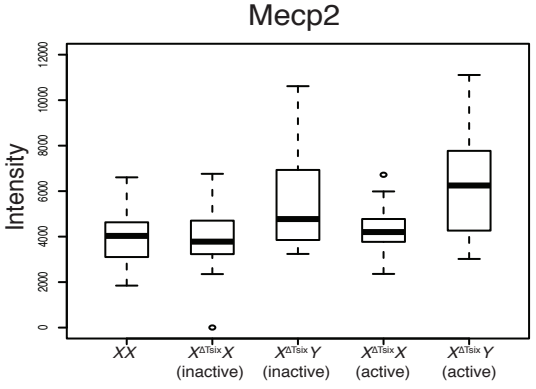
Mecp2
Intensity
0
2000
4000
6000
8000
10000
12000
XX
X^ΔTsix X (inactive)
X^ΔTsix Y (inactive)
X^ΔTsix X (active)
X^ΔTsix Y (active)

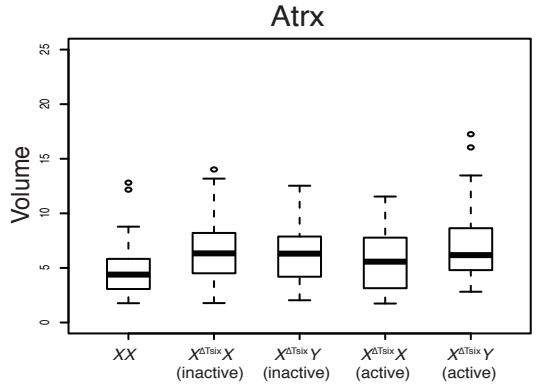
Atrx
Volume
0
5
10
15
20
25
XX
X^ΔTsix X (inactive)
X^ΔTsix Y (inactive)
X^ΔTsix X (active)
X^ΔTsix Y (active)

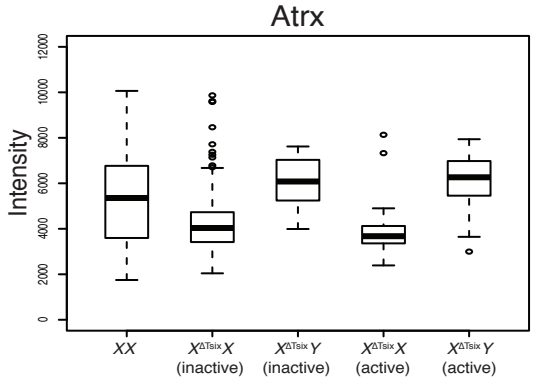
Atrx
Intensity
0
2000
4000
6000
8000
10000
12000
XX
X^ΔTsix X (inactive)
X^ΔTsix Y (inactive)
X^ΔTsix X (active)
X^ΔTsix Y (active)

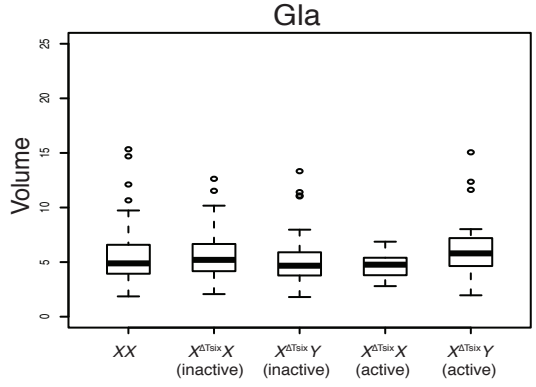
Gla
Volume
0
5
10
15
20
25
XX
X^ΔTsix X (inactive)
X^ΔTsix Y (inactive)
X^ΔTsix X (active)
X^ΔTsix Y (active)

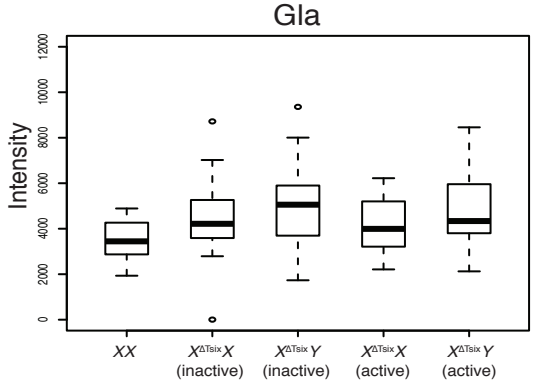
Gla
Intensity
0
2000
4000
6000
8000
10000
12000
XX
X^ΔTsix X (inactive)
X^ΔTsix Y (inactive)
X^ΔTsix X (active)
X^ΔTsix Y (active)

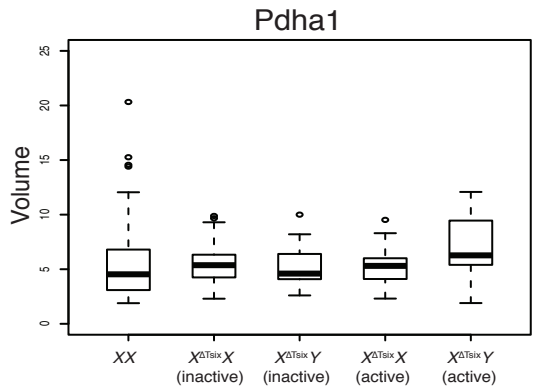
Pdha1
Volume
0
5
10
15
20
25
XX
X^ΔTsix X (inactive)
X^ΔTsix Y (inactive)
X^ΔTsix X (active)
X^ΔTsix Y (active)

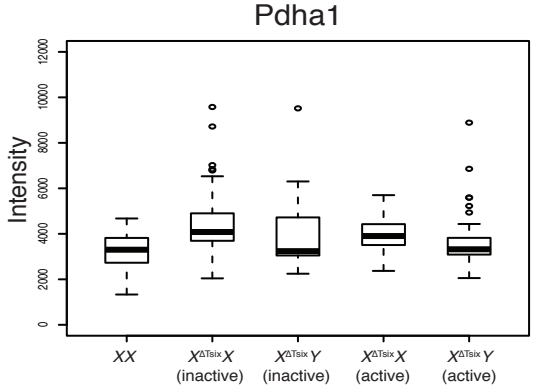
Pdha1
Intensity
0
2000
4000
6000
8000
10000
12000
XX
X^ΔTsix X (inactive)
X^ΔTsix Y (inactive)
X^ΔTsix X (active)
X^ΔTsix Y (active)

Figure S11. Volume and intensity of Xist RNA coats in $X^{\Delta Tsix}Y$, XX, and $X^{\Delta Tsix}X$ EpiSCs. Boxplots of automated 3D measurements of volume (left) and intensity (right) of Xist RNA coats coincident with expression (active) or silencing (inactive) of the X-linked genes *Lamp2*, *Mecp2*, *Atrx*, *Gla*, and *Pdha1*. Boxplots show the median percent gene expression (line), second to third quartiles (box), and 1.5X the interquartile range (whiskers). Two different lines were analyzed for each genotype (*XX* lines 1-2; $X^{\Delta Tsix}Y$ lines 1-2; $X^{\Delta Tsix}X$ lines 4 and 5; all from Fig. 3); both sets of measurements of Xist RNA coats coincident with expression or silencing occurred on the same samples, thus minimizing variability of stains. Volume and intensity of Xist RNA clouds were compared between pairs of samples, divided by sex and gene expression status (female inactive vs. male inactive; female active vs. male active) using a one-tailed T-test, testing the assumption that Xist clouds in males would show lower volume and decreased intensity of signal compared to those in female cells. No statistically significant difference in either measurement was found between mutant males vs. WT or mutant females ($p > 0.025$). n=50 nuclei/cell line.

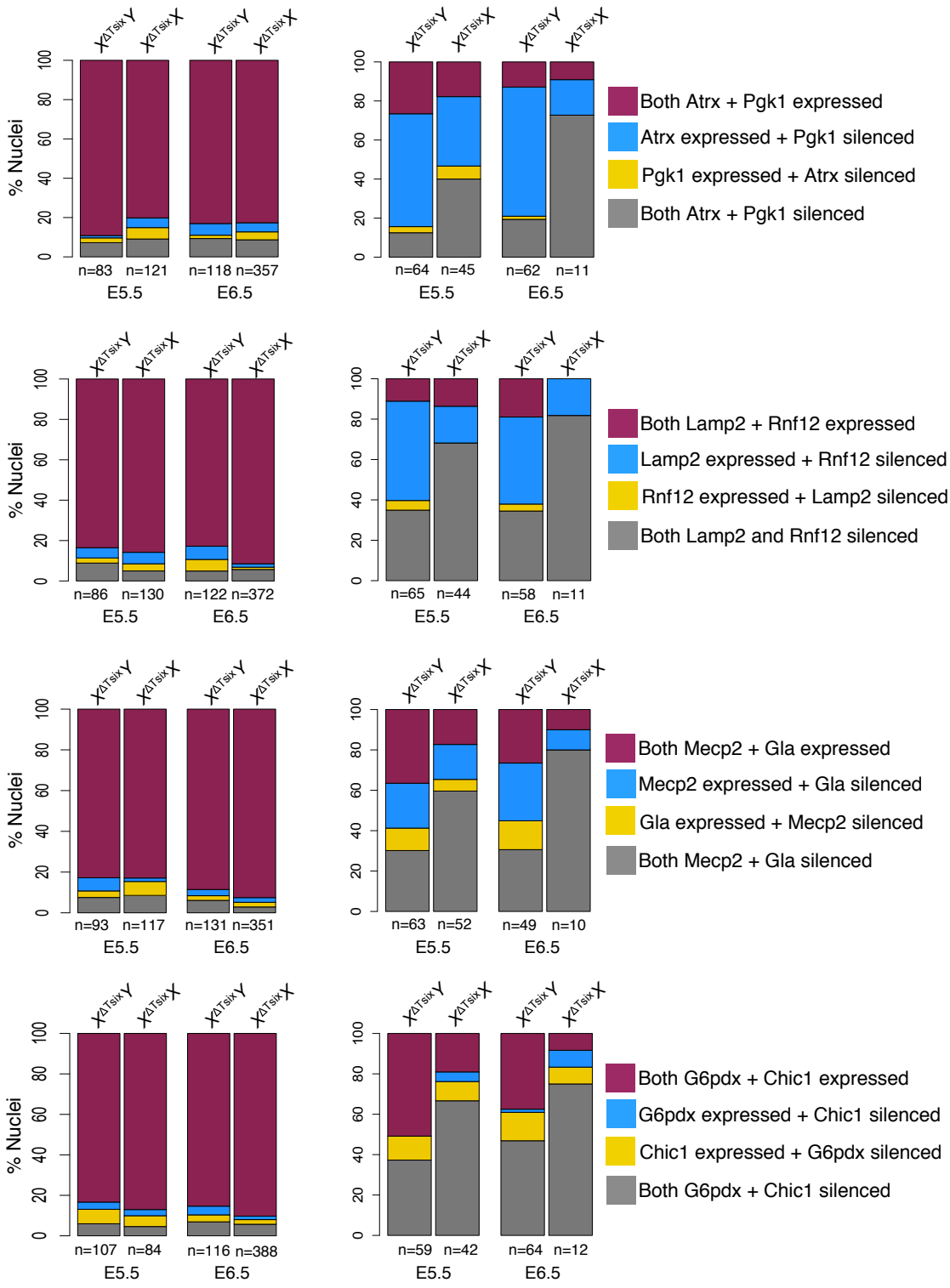
% Nuclei
0
20
40
60
80
100
XΔTsixY
XΔTsixX
n=83 n=121 n=118 n=357
E5.5 E6.5
n=64 n=45 n=62 n=11
E5.5 E6.5
Both Atrx + Pgk1 expressed
Atrx expressed + Pgk1 silenced
Pgk1 expressed + Atrx silenced
Both Atrx + Pgk1 silenced
n=86 n=130 n=122 n=372
E5.5 E6.5
n=65 n=44 n=58 n=11
E5.5 E6.5
Both Lamp2 + Rnf12 expressed
Lamp2 expressed + Rnf12 silenced
Rnf12 expressed + Lamp2 silenced
Both Lamp2 and Rnf12 silenced
n=93 n=117 n=131 n=351
E5.5 E6.5
n=63 n=52 n=49 n=10
E5.5 E6.5
Both Mecp2 + Gla expressed
Mecp2 expressed + Gla silenced
Gla expressed + Mecp2 silenced
Both Mecp2 + Gla silenced
n=107 n=84 n=116 n=388
E5.5 E6.5
n=59 n=42 n=64 n=12
E5.5 E6.5
Both G6pdx + Chic1 expressed
G6pdx expressed + Chic1 silenced
Chic1 expressed + G6pdx silenced
Both G6pdx + Chic1 silenced

Figure S12. Ectopic Xist induction and X-linked gene silencing in post-implantation $X^{\Delta Tsix}Y$ and $X^{\Delta Tsix}X$ embryos. Barplots assessing expression pattern of the four pairs of genes analyzed by RNA FISH in Tsix-mutant embryonic epiblasts X-linked gene expression was quantified both in nuclei without (left) and with (right) ectopic Xist RNA coating. For pairs of genes exhibiting differential levels of silencing, the two genes are discordantly silenced more frequently in $X^{\Delta Tsix}Y$ vs. $X^{\Delta Tsix}X$ epiblasts. In nuclei with ectopic Xist RNA coating, all genes except *Pgk1* and *Rnf12* are silenced significantly more often in females compared to males (*Atrx*, *Lamp2*, *Mecp2*, *Gla*, *G6pdx*, and *Chic1*, $p < 0.01$ at E5.5 and $p < 0.05$ at E6.5; *Pgk1*, $p = 0.7$ at E5.5 and $p = 1$ at E6.5; *Rnf12*, $p = 0.80$ at E5.5 and 0.2 at E6.5; Fisher's exact test). Related to Fig. 6.

Table S1

X-linked Gene Silencing Upon Ectopic Xist RNA Coating
$X^{\Delta Tsix}Y$ vs. $X^{\Delta Tsix}X$ ESCs

Gene	D4	D6	D8
Lamp2	$p < 0.01$	$p < 0.01$	$p < 0.001$
Mecp2	$p < 0.05$	$p < 0.01$	$p < 0.01$
G6pdx	$p < 0.01$	$p < 0.01$	$p < 0.05$
Chic1	$p < 0.01$	$p < 0.01$	$p < 0.01$
Rnf12	$p < 0.01$	$p < 0.01$	$p < 0.05$
Atrx	$p < 0.001$	$p < 0.01$	$p < 0.01$
Pgk1	$p < 0.05$	$p < 0.05$	$p < 0.05$
Gla	$p < 0.05$	$p < 0.05$	$p < 0.05$
Pdha1	$p < 0.01$	$p < 0.05$	$p < 0.001$
Smcx	$p < 0.01$	$p < 0.01$	$p < 0.001$

Supplemental Table 1. P-values from T-tests comparing X-linked gene silencing in differentiating $X^{\Delta Tsix}Y$ and $X^{\Delta Tsix}X$ ESCs. $p = 0.05$ was used as the cutoff for statistical significance. D, day or differentiation.

Table S2

X-linked Gene Silencing Upon Ectopic Xist RNA Coating
$X^{\Delta Tsix}Y$ vs. $X^{\Delta Tsix}O$ ESCs

Gene	D4	D6	D8
Lamp2	NS	NS	NS
Mecp2	NS	NS	NS
G6pdx	NS	NS	NS
Chic1	NS	NS	NS
Rnf12	NS	NS	NS
Atrx	NS	NS	NS
Pgk1	NS	NS	NS
Gla	NS	NS	NS
Pdha1	NS	NS	NS
Smcx	NS	NS	NS

X-linked Gene Silencing Upon Xist RNA Coating
$X^{\Delta Tsix}X$ vs. $X^{\Delta Tsix}O$ ESCs

Gene	D4	D6	D8
Lamp2	$p < 0.001$	$p < 0.01$	$p < 0.001$
Mecp2	$p < 0.01$	$p < 0.01$	$p < 0.01$
G6pdx	$p < 0.01$	$p < 0.01$	$p < 0.01$
Chic1	$p < 0.001$	$p < 0.01$	$p < 0.05$
Rnf12	$p < 0.01$	$p < 0.01$	$p < 0.05$
Atrx	$p < 0.01$	$p < 0.01$	$p < 0.01$
Pgk1	$p < 0.05$	$p < 0.05$	$p < 0.05$
Gla	$p < 0.01$	NS	$p < 0.05$
Pdha1	$p < 0.01$	$p < 0.05$	$p < 0.05$
Smcx	$p < 0.01$	$p < 0.01$	$p < 0.001$

Supplemental Table 2. P-values from T-tests comparing X-linked gene silencing in differentiating $X^{\Delta Tsix}Y$ and $X^{\Delta Tsix}X$ to gene silencing in differentiating $X^{\Delta Tsix}O$ ESCs. $p = 0.05$ was used as the cutoff for statistical significance. NS, not significant. D, day or differentiation.

Table S3

X-linked Gene Silencing Upon Ectopic Xist RNA Coating
$X^{\Delta Tsix}Y$ vs. $X^{\Delta Tsix}X$ EpiSCs

Gene	D5	D10	D15
Lamp2	$p < 0.001$	$p < 0.001$	$p < 0.001$
Mecp2	$p < 0.001$	$p < 0.001$	$p < 0.001$
G6pdx	$p < 0.001$	$p < 0.001$	$p < 0.001$
Chic1	$p < 0.001$	$p < 0.001$	$p < 0.001$
Rnf12	$p < 0.001$	$p < 0.001$	$p < 0.001$
Atrx	$p < 0.001$	$p < 0.001$	$p < 0.001$
Pgk1	$p < 0.001$	$p < 0.01$	$p < 0.01$
Gla	$p < 0.001$	$p < 0.001$	$p < 0.001$
Pdha1	$p < 0.001$	$p < 0.001$	$p < 0.001$
Smcx	$p < 0.001$	$p < 0.001$	$p < 0.001$

Supplemental Table 3. P values from T-tests comparing X-linked gene silencing in differentiating $X^{\Delta Tsix}Y$ and $X^{\Delta Tsix}X$ EpiSCs. $p = 0.05$ was used as the cutoff for statistical significance. D, day or differentiation.

SUPPORTING INFORMATION MATERIALS & METHODS

Mice. The generation of mice harboring the *Tsix*$^{AA2\Delta1.7}$ mutation has been described previously (1-3). The JF1 strain has also been described previously (3, 4).

Embryo Dissections and Processing. Pre-, peri-, and post-implantation stage embryos were isolated essentially as described (5). Dissections were carried out in 1X PBS (Invitrogen, #14200075) containing 6% bovine serum albumin (BSA; Invitrogen, #15260037). Individual implantation sites were cut from the uterine limbs, and decidua were removed with forceps. Embryos were dissected from the decidua, and the Reichert's membranes surrounding post-implantation embryos were removed using fine forceps. For separation of extra-embryonic and epiblast portions of embryos, fine forceps were used to physically bisect the embryos at the junction of the extra-embryonic ectoderm and epiblast. Epiblast fragments were plated on gelatinized coverslips for immunofluorescence and/or RNA FISH or collected for mRNA extraction. Extra-embryonic portions of the embryo were lysed to extract DNA to confirm sex and genotype.

Derivation, Culture and Differentiation of Embryonic Stem Cell (ESCs) Lines. ESC lines were derived following the protocol previously described (6), and have been characterized previously (7). Cells were cultured in Knockout DMEM (GIBCO, #10829-018) with 15% Knockout Serum Replacement (GIBCO, #A1099201), 5% FBS (GIBCO, #104390924), 2 mM L-glutamine (GIBCO, #25030), 0.1 mM 2-mercaptoethanol (Sigma, #M7522), 1X nonessential amino acids (GIBCO, #11140-050), and 103 units/mL LIF (Millipore #ESG1106). Cells were differentiated by forming embryoid bodies in

suspension culture without LIF as previously described (8) for one day, then plated onto gelatinized plates or coverslips. The $X^{\Delta Tsix}O$ ESC lines were subcloned from $X^{\Delta Tsix}X$ ESC line 2.

Derivation, Culture and Differentiation of Epiblast Stem Cell (EpiSC) Lines. EpiSCs were derived following the protocol described previously (9-11), and have been characterized previously (7). Cells were cultured in a medium containing Knockout DMEM supplemented with 20% KSR, 2 mM Glutamax (GIBCO, #35050061), 1X nonessential amino acids, 0.1 mM 2-mercaptoethanol, and 10 ng/ml FGF2 (R&D Systems, #233-FB). EpiSCs were passaged every third day using 1.5 mg/ml collagenase type IV (GIBCO, #17104-019) with pipetting into small clumps. Differentiation of EpiSCs was achieved by growing the EpiSCs on gelatin-coated tissue culture dishes in EpiSC medium lacking FGF2.

For IF and/or RNA FISH, EpiSCs were cultured on gelatin-coated glass coverslips. The cells were then permeabilized through sequential treatment with ice-cold cytoskeletal extraction buffer (CSK:100 mM NaCl, 300 mM sucrose, 3 mM MgCl2, and 10 mM PIPES buffer, pH 6. 8) for 30 sec, ice-cold CSK buffer containing 0.4% Triton X-100 (Fisher Scientific, #EP151) for 30 sec, followed twice with ice-cold CSK for 30 sec each. After permeabilization, cells were fixed by incubation in 4% paraformaldehyde for 10 min. Cells were then rinsed 3X in 70% ethanol and stored in 70% ethanol at -20°C prior to IF and/or RNA FISH.

RNA Fluorescence *in situ* Hybridization (RNA FISH). Double-stranded RNA FISH (dsRNA FISH) was performed as previously described (2, 4, 12). The dsRNA FISH

probes were made by randomly-priming DNA templates using BioPrime DNA Labeling System (Invitrogen, #18094011). Probes were labeled with Fluorescein-12-dUTP (Invitrogen), Cy3-dCTP (GE Healthcare, #PA53021). Labeled probes from multiple templates were precipitated in a 0.3M sodium acetate solution (Teknova, #S0298) along with 300 μg of yeast tRNA (Invitrogen, #15401-029) and 150 μg of sheared, boiled salmon sperm DNA (Invitrogen, #15632-011). The solution was then spun at 15,000 rpm for 20 min at 4°C. The pellet was washed consecutively with 70% ethanol and 100% ethanol. The pellet was dried and re-suspended in deionized formamide (ISC Bioexpress, #0606). The probe was denatured by incubating at 90°C for 10 min followed by an immediate 5 min incubation on ice. A 2X hybridization solution consisting of 4X SSC, 20% Dextran sulfate (Millipore, #S4030), and 2.5 mg/ml purified BSA (New England Biolabs, #B9001S) was added to the denatured solution. All probes were stored at -20°C until use.

Strand-specific RNA FISH (ssRNA FISH) probes were labeled with Cy5 CTP (GE Healthcare, # 25801086) or Cy3 CTP (GE Healthcare, # 25801086) using Invitrogen MAXIscript Kit (Invitrogen, #AM-1324). Labeled probes were column purified (Roche, #11814427001) and precipitated in an 0.25M ammonium acetate solution as described above for the dsRNA FISH probes. Probes were resuspended as described for dsRNA FISH probes and stored at -20°C.

Cells or embryo fragments mounted on coverslips were dehydrated through 2 min incubations in 70%, 85%, 95%, and 100% ethanol solutions and subsequently air-dried. The coverslips were then hybridized to the probe overnight in a humid chamber at 37°C.

The samples were then washed 3X for 7 min each while shaking at 39°C with 2XSSC/50% formamide, 2X with 2X SSC, and 2X with 1X SSC. A 1:250,000 dilution of DAPI (Invitrogen, #D21490) was added to the third 2X SSC wash. The cells were then mounted in Vectashield (Vector Labs, #H-1200).

DNA FISH. After RNA FISH, the cells were washed with 1X PBS three times and then incubated in PBS for 5 min at room temperature. The cells were then refixed with 1% (wt/vol) PFA containing 0.5% (vol/vol) Tergitol and 0.5% (vol/vol) Triton X-100 for 10 min at room temperature. The cells were next dehydrated through an ethanol series (70%, 85%, and 100% ethanol, 2 min each) and air dried for 15 mins. The cells were then treated with RNase A (1.25 μg/μl) at 37^0C for 30 min. The cells were again dehydrated through the ethanol series as described above. The samples were then denatured in a prewarmed solution of 70% formamide in 2X SSC on a glass slide stationed on top of a heat block set at 95°C for 11 min followed immediately by dehydration through a -20°C-chilled ethanol series (70%, 85%, 95%, and 100% ethanol, 2 min each). The cells were then air dried for 15 min followed by probe hybridization overnight at 37^0C. The BAC template used for Xist DNA FISH is RP24-287F13 (Children's Hospital of Oakland Research Institute). The next day, the samples were washed twice with prewarmed 50% formamide/2X SSC solution at 39^0C and 2X with 2X SSC, 7 min each.

Immunofluorescence (IF). Cells mounted on glass coverslips were washed 3X in PBS for 3 min each while shaking. Coverslips were then incubated in blocking buffer consisting of 0.5 mg/mL BSA (New England Biolabs, #B9001S), 50 μg/mL yeast tRNA

(Invitrogen, #15401-029), 80 units/mL RNAseOUT (Invitrogen, #10777-019), and 0.2% Tween 20 (Fisher, #BP337-100) in 1X PBS in a humid chamber for 30 min at 37°C. The samples were next incubated with primary antibody diluted in blocking buffer for 1 hr in the humid chamber at 37°C. The H3-K27me3 antibody (Millipore, #07-449) was used at a 1:2500 dilution. The samples were then washed 3X in PBS/0.2% Tween 20 for 3 min each while shaking. After a 5 min incubation in blocking buffer at 37°C in the humid chamber, the samples were incubated in blocking buffer containing a 1:300 dilution of fluorescently-conjugated secondary antibody (Alexa Fluor, Invitrogen) for 30 min in the humid chamber at 37°C, followed by three washes in PBS/0.2% Tween 20 while shaking for 3 min each. The samples were then processed for RNA FISH.

Quantification of Allele-specific Expression by Pyrosequencing.

Allele-specific expression of Xist was quantified using Qiagen PyroMark sequencing platform. Xist amplicon containing a single nucleotide polymorphism (SNP) were designed using the PyroMark Assay Design software. Single cell lysates were prepared using 5 μL of lysis buffer from the Single Cell RT-PCR Assay Kit by Signosis (# CL-0002). The 5 μl cell lysate was used directly for cDNA synthesis. cDNA synthesis was performed using the Invitrogen SuperScript III One-Step RT-PCR System (# 12574-026). Following the PCR reaction, 5 μl of a total of 25 μL was run on a 3% agarose gel to assess the efficacy of the reverse transcription and amplification. The samples were then prepared for Pyrosequencing according to the standard recommendations for use with the PyroMark Q96 ID sequencer. The Xist amplicon spanned intron 2 thus excluding any amplified contaminating genomic DNA sequence due to size differences. The following primers were used in Xist RT-PCR: forward, CAAGAAGAAGGATTGCCTGGATTT;

reverse, 5'-biotin-GCGAGGACTTGAAGAGAAGTTCTG; sequencing, CAAACAATCCCTATGTGA.

Cell Proliferation and Viability. Live/Dead cell viability assay (Life technologies cat. #L3224) was performed as described previously in Gayen et al., (2015). 50,000 EpiSCs were plated on gelatinized plate and differentiated as described above. Cells were counted using the Trypan blue (Invitrogen cat. #15250061) exclusion assay with Invitrogen Countess Automated Cell Counter (cat. # C10227). Cell viability was calculated both for adherent cells, harvested via trypsinization, and cells in suspension, harvested by centrifugation of culture media. Data were collected from three independent differentiation experiments.

Microscopy. Images of all stained samples were captured using a Nikon Eclipse TiE inverted microscope build with a Photometrics CCD camera. The images were analyzed after deconvolution using NIS-Elements software. All images were processed uniformly. The volume and intensity of Xist RNA signals were measured using the NIS elements "3D Measurement; 3D thresholding, 3D viewing and voxel based measurements" software package (Nikon Instruments, 77010582). Briefly, the fluorescence channel with the Xist RNA FISH stain was extracted from each image, and uniform thresholds were set for signal size and intensity across all images to avoid inclusion of background signal. For all regions above threshold within an image, the volume and signal intensity of each discrete region was calculated.

Supporting Information References

1. Sado T, Wang Z, Sasaki H, & Li E (2001) Regulation of imprinted X-chromosome inactivation in mice by Tsix. *Development* 128(8):1275-1286.

2. Kalantry S & Magnuson T (2006) The Polycomb group protein EED is dispensable for the initiation of random X-chromosome inactivation. *PLoS Genet* 2(5):e66.

3. Maclary E*, et al.* (2014) Differentiation-dependent requirement of Tsix long non-coding RNA in imprinted X-chromosome inactivation. *Nat Commun* 5:4209.

4. Kalantry S, Purushothaman S, Bowen RB, Starmer J, & Magnuson T (2009) Evidence of Xist RNA-independent initiation of mouse imprinted X-chromosome inactivation. *Nature* 460:647-651.

5. Hogan B (1994) *Manipulating the mouse embryo : a laboratory manual* (Cold Spring Harbor Laboratory Press, Plainview, N.Y.) 2nd Ed pp xvii, 497 p.

6. Bryja V, Bonilla S, & Arenas E (2006) Derivation of mouse embryonic stem cells. *Nat Protoc* 1(4):2082-2087.

7. Gayen S, Maclary E, Buttigieg E, Hinten M, & Kalantry S (2015) A Primary Role for the Tsix lncRNA in Maintaining Random X-Chromosome Inactivation. *Cell reports* 11(8):1251-1265.

8. Hopfl G, Gassmann M, & Desbaillets I (2004) Differentiating embryonic stem cells into embryoid bodies. *Methods Mol Biol* 254:79-98.

9. Najm FJ*, et al.* (2011) Isolation of epiblast stem cells from preimplantation mouse embryos. *Cell Stem Cell* 8(3):318-325.

10. Tesar PJ*, et al.* (2007) New cell lines from mouse epiblast share defining features with human embryonic stem cells. *Nature* 448(7150):196-199.

11. Brons IG*, et al.* (2007) Derivation of pluripotent epiblast stem cells from mammalian embryos. *Nature* 448(7150):191-195.

12. Kalantry S*, et al.* (2006) The Polycomb group protein Eed protects the inactive X-chromosome from differentiation-induced reactivation. *Nat Cell Biol* 8(2):195-202.